Journal of the Korean Society of
Tobacco Science. Vol. 18 No.1, 92~99(1996)
Printed in Republic of Korea.

Pressure Gradient of Supercritical CO_2 in Vertical Tobacco Beds in Down Flow Condition

Sung Chul Yi*
Department of Chemical Engineering, HanYang University
(Received March 15, 1996)

담배 고정층 반응기에서 하부로 흐르는 초임계 CO_2의 압력 구배

이 성 철*
한양대학교 화학공학과
(1996년 3월 15일 접수)

ABSTRACT : A mathematical model of the pressure gradient of supercritical CO_2 in a vertical tobacco bed was developed in this study. In particular, the compaction of the tobacco as a function of temperature and CO_2 flow is included in the model. Downflow of CO_2 flow condition is described. At velocities in excess of 0.6 cm/sec at 70℃, there is a large increase in pressure gradient for beds deeper than about 0.5 m. The proposed model offers a better understanding of operating the process using supercritical CO_2.
***Key words**: mathematical model, supercritical CO_2, tobacco bed*

Expanded tobacco provides increased filling power in cigarettes by decreasing the bulk density of the fill material. Most of the present popular brands selling in the market contain approximately 10% expanded tobacco in the total blend. It is anticipated that future brands of cigrettes

* 연락저자 : 133-791, 서울특별시 성동구 행당동 17번지, 한양대학교 화학공학과
* Corresponding Author : *Dept. of Chemical Engineering, Hanyang University, 17, Haengdang-Dong, Sungdong-Ku, Seoul 133-791, Korea*

ill be developed that will contain a much higher percentage of expanded tobacco. One of the techn-ique the expanded tobacco is supercritical CO_2 vased process, which often operates in a vertical tobacco bed. To achieve the optimal operating condition, knowledge of CO_2 behavior in the bed is essential. A mathematical model for the pressure gradient of supercritical CO_2 across vertical tobacco bed is developed to understand the phenomena. Experimental observations were indicating that as flow rate was increased, the pressure gradient was increasing far beyond expected levels. Furthermore, the bed of tobacco was noted to be collapsing into a very dense mass near the bottom of the bed. However, the collapse was non-linear so that the average density was moderate.

The model including a model for tobacco compressibility has been developed which has all of the required attributes to reflect the process observ-ations. This model has allowed us to explore the effects of tobacco charge weight, initial density, initial height, and flow rate.

Theory

The compression of tobacco has been shown to be described by:

$$P(x) = K(\rho^3 - \rho_m^3), \tag{1}$$

where P(x) is the mechanical pressure on a bed of tobacco whose density is p, and the density p_m is the threshold density (minimum) to support a load. The quantity p_m is set to zero.

Equation (1) was adapted to the flow model in the following way to be described. Equation (1) was incorporated in differential form to the gradient for the total mechanical pressure on a differential of the tobacco bed where the mechanical pressure is defined in equation (2) with the coordinate system in the following Figure 1 for the down flow case:

$$P(x) = g\left(1 - \frac{\rho_{co_2}}{\rho_m}\right)\int_0^x \rho(x')dx' + p(0) - p(x), \tag{2}$$

where P(x) is the total mechanical pressure on the element dx at position x, and p(0) and p(x) are the fluid pressure at the top and position x in the bed. Then, first term in right hand side of equation (2) is the net gravitational pressure including buoyancy in the fluid on the element dx and the term, p(0)-p(x), is the pressure drop of the fluid across the bed over the distance x.

The fluid velocity V in Figure 1 is in the same direction as grvity. The densities ρ_{mt} and ρ_{CO2} are that of the mass density of the shreds in the CO_2 and the fluid density of the CO_2, respectively.

The gradient in mechanical pressure is then obtained in equation (3):

$$\frac{dP(x)}{dx} = g\left(1 - \frac{\rho_{co_2}}{\rho_m}\right)\rho(x) - \frac{dp}{dx}. \tag{3}$$

However, the total mechanical pressure gradient is related to the mechanical properties of the tobacco bed through the gradient in equation (1) using the chain rule:

$$\frac{dP(x)}{dx} = \frac{dP(x)}{d\rho(x)}\frac{d\rho(x)}{dx} = 3K\rho^2(x)\frac{d\rho(x)}{dx} = \alpha\rho^2(x)\frac{d\rho(x)}{dx}. \tag{4}$$

The relationship between the fluid pressure p, its velocity, and the properties of the tobacco bed must next be determined. For that relationship, the Ergun equation, described in Bird et al. (1960), is used:

$$\frac{dp}{dx} = -a(\rho)v - b(\rho)v^2, \tag{5}$$

where equation (5) is the Ergun equation and the parameters $a(\rho)$ and $b(\rho)$ are the same as those

described in Bird et al.(1960). Thus, the fluid pressure depends upon the drag created by the bed. The drag is function of bed density (porosity), surface area of the bed, and roughness of the individual shreds. The velocity V is the face velocity of the fluid. Form this point, equation (5), the suffix (x) will be dropped, but dependency on x is understood.

Equations (4) and (5) are substituted into equation (3) which is rearranged to yield the desired relationship for the density gradient given in equation (6).

$$\frac{d\rho}{dx} = \frac{1}{\alpha\rho^2}\left\{g\left[\rho_{mt} - \rho_{co_2}\right]\frac{\rho}{\rho_{mt}} + \left[a(\rho)v + b(\rho)v^2\right]\right\}. \qquad (6)$$

Finally, equation (6) is generalized by scaling the variables in the following manner:

$$x^* = x/\alpha,$$
$$p^* = p/\alpha.$$

Using the scaled variables leads to the generalized forms of equations (3) and (6):

$$\frac{dp^*}{dx^*} = -a(\rho)v - b(\rho)v^2 \qquad (7a)$$

$$\frac{d\rho}{dx^*} = \frac{1}{\rho^2}\left\{g\left(\rho_{mt} - \rho_{co_2}\right)\frac{\rho}{\rho_{mt}} + \left[a(\rho)v + b(\rho)v^2\right]\right\} \qquad (7b)$$

Equations (7) were converted to forward, explicited finite different forms and solved numerically for pressure p and density ρ. The aerodynamic density of the tobacco shreds was assumed to be 1.0g/cc which corresponds to the excluded geometric volume of the shreds and ρ_{mt} as assumed to be 1.45g/cc obtained from measurements in CO_2. The aerodynamic density was used to calculate the bed interstitial porosity. The total porosity including that within the shreds is related to the interstitial porosity by equations (8):

$$\varepsilon_a = \frac{\rho_a - \rho}{\rho_a} \qquad (8a)$$

$$\varepsilon_b = \frac{1.0 - \rho}{1.0} \qquad (8b)$$

$$\varepsilon_t = \frac{1.45 - \rho}{1.45} \qquad (8c)$$

$$1 - \varepsilon_t = \frac{\rho}{1.45} \qquad (8d)$$

where ρ_a is excluded volume density (aerodynamic) or true density, ε_b and ε_t are interstitial and total porosity, respectively, and ρ is the calculated bed density from equation (7b). The excluded volume density and true density of the shreds were used in equations (8b) and (8c), respectively.

The porosity of the individual shreds, due to their internal void space, has an effect on the buoyancy of the shreds. The more permeable the internal void spaces are to the suspending liquid, the greater the apparent internal void volume and the higher the actual density of the mass of tobacco in the shred. However, the excluded volume, defined as the volume based on the shred boundaries and measured with a nonpenetrating liquid, is unaffected. Thus, the drag terms are unaffected by the internal voids of the individual shreds. Based on the experimental data for tobacco in supercritical CO_2, the estimated true density of tobacco in this fluid is 1.45g/cc obtained via Beckmann aerometer as compared to the 1.00 g/cc based on its exculuded volume from acetone measurements. The result is an apparent increase in the bulk modulus from 3.4E5 with a true tobacco density of 1.0g/cc(based on excluded volume) to 6.98E5 at 1.45g/cc (based on supercritical experiments).

Finally, one must also consider conservation of mass in order to relate the pressure drop and bed density to an initial bed weight(charge) W_0, density and height. Equations (9) describe the relationships:

$$W_0 = A \cdot Dx \sum \rho_i = A \cdot LO \cdot \rho_0 \quad (9a)$$

$$W_0 = A \cdot Dx = A \cdot LO \cdot \rho_{avg} \cdot xl \quad (9b)$$

$$\rho_{avg} \cdot xl = \rho_0 \cdot LO \quad (9c)$$

$$xl = \sum Dx \quad (9d)$$

where ρ_0, ρ_{avg}, and ρ_i are initial, average and position densities, respectively. The distance LO, xl, and Dx are initial bed height, bed height at position x, and incremental distance in a bed of cross-sectional area A. By constantly comparing the average density-distance product to that of the initial bed density-bed height product (total initial charge), one can determine the final equilibrium bed height corresponding to the initial charge:

$$RATM = \frac{\rho_{avg} \cdot xl}{\rho_o \cdot LO} \quad (10a)$$

$$RATM = 1.0 = \frac{\rho_{avg} \cdot xle}{\rho_o \cdot LO} \quad (10b)$$

where the product ratio RATM equals 1.0 at equilibrium and the final equilibrium bed depth is xle. The bed depth xle is the depth to which a bed of initial weight W_0 packed to an height LO and initial density ρ_0 is compressed at a given CO_2 flow and velocity.

Results and Discussion

Solutions for pressure p and density ρ for various initial values of modulus, bed density, bed height, and charge were determined at several flow rates including zero flow. The model agrees well with the experimental data (Simpson, 1986). The results were plotted according to the prescribed form to factor out the modulus α. Therefore, p/x of the fluid and ρ were plotted, respectively, versus x/α as shown in Figures 1-9 for the various parameters. The plots versus x/α are independent of α for general solutions which can be used to estimate α if pressure p and equilibrium depth x are known. However, an initial estimate of α is better to obtain a scale for numerical solutions and plotting convenience. The pressure volume data obtained for cut filler at 25℃ as a function of oven volatile (OV) in the 14-25% range with the Instron was used as a starting value. Using the slope K at OV equal to 25%, and noting that α is equal to 3 times K, the value of α at 25℃ is 2.064×10^7 (dynes/cm^2) /(g/cc)^3. By matching the experimentally observed pressure gradients and depths at 0.3, 0.6, and 1.0 cm/sec at 70℃ which is the process operating temperature, an initial estimate of $\alpha = 6.98 \times 10^5$ (dynes/cm^2)/(g/cc)^3 is obtained. The only value affected by α is the equilibrium depth corres- ponding to a given initial density or height. That is the degree of compression, and, consequently the final density and pressure gradient are determined by α, initial density, bed height, flow velocity, fluid density, and fluid viscosity, and gravity. The value of α is moisture dependent, and by temperature as the experimental data at 25℃ and 70℃ indicate. This dependence on temperature may be a result of a postulated glass transitional temperature observed in tobacco filler heat capacity studies. It was shown that a transition in heat capacity occurs at 47℃ for filler at about 8% OV and decreases as moisture level increases. A glassy transition would cause tobacco to be much softer at temperatures in excess of the transition temperature than below it.

At 70℃, the Figures demonstrate a very large compression of tobacco even at zero flow where gravity corrected for buoyancy is acting on the bed. At 0.3 cm/sec, the pressure gradient is not as severe as at 0.6 or 1.0 cm/sec nor is the

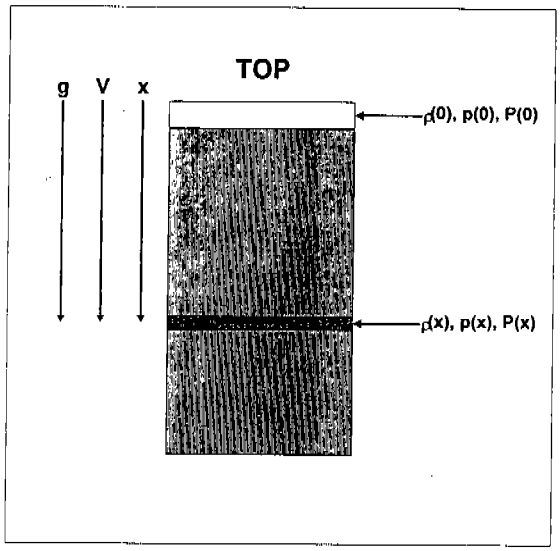

Fig. 1. Schematic diagram of local and mechanical pressures in tobacco bed for downflow

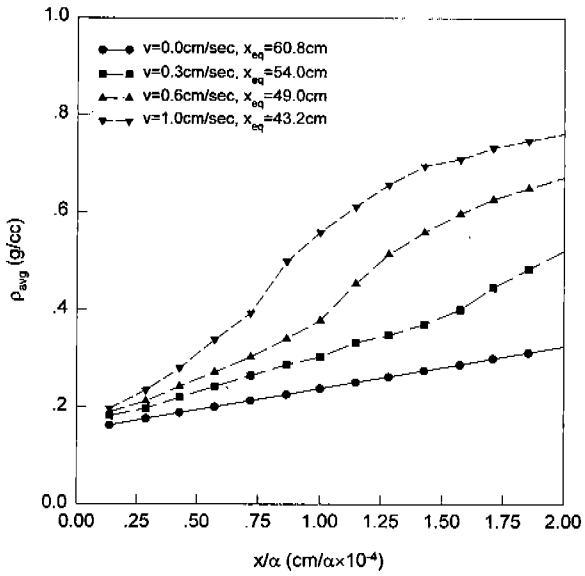

Fig. 3. Average density vs. depth / α at equillibrium for various velocities. (ρ_T=1.45g/cc, α=6.98×10^5 dyne/cm^2/(g/cc)^3, 70℃, ρ(0)=0.15g/cc, 1M)

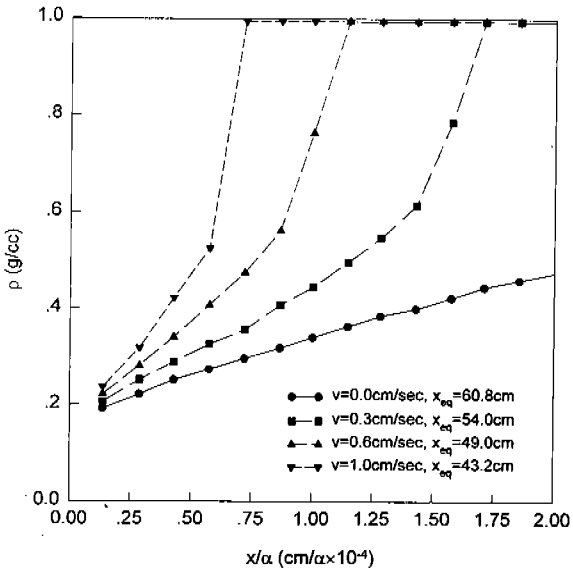

Fig. 2. Density vs. depth/α at equillibrium for various velocities (ρ_T=1.45g/cc, α=6.98×10^5 dyne/ cm^2/(g/cc)^3, 70℃, ρ(0)=0.15g/cc, 1M)

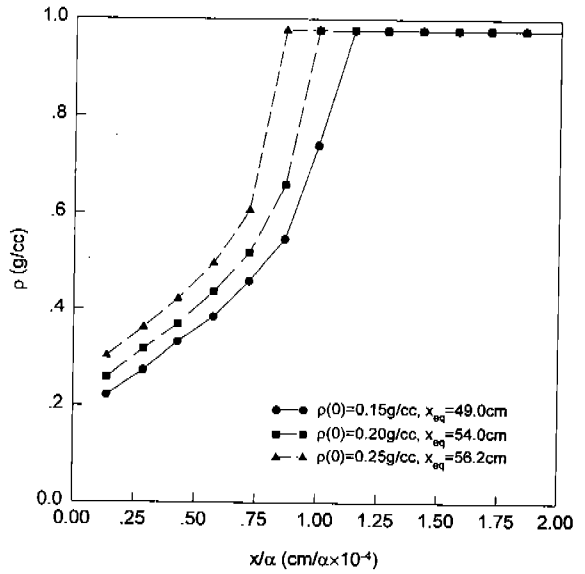

Fig. 4. Density vs. depth/α at equillibrium for various initial charge densities. (ρ_T=1.45 g/cc, α=6.98×10^5 dyne/cm^2/(g/cc)^3, 70℃, v=0.6 cm/sec, 1M)

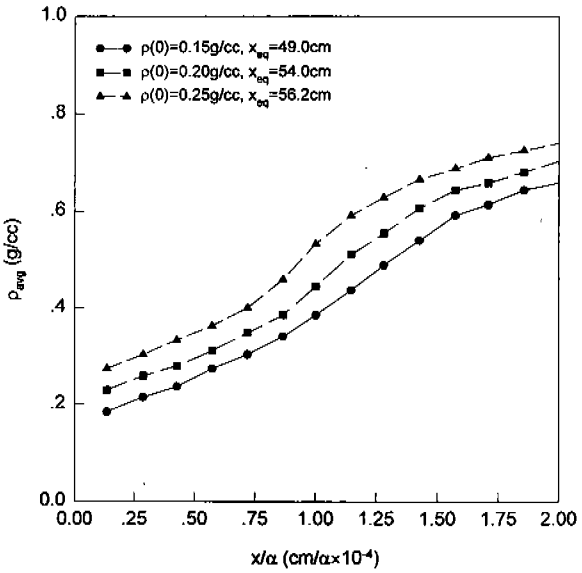

Fig. 5. Average density vs. depth/α at equillibrium for various initial charge densities. (ρ_T=1.45 g/cc, $\alpha=6.98\times10^5$ dyne/cm^2/(g/cc)^3, 70℃, v=0.6 cm/sec, 1M)

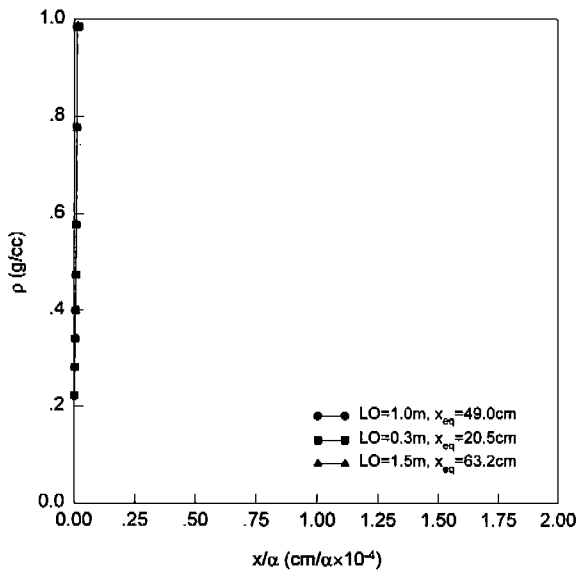

Fig. 6. Density vs. depth/α at equillibrium for various tobacco bed heights. (ρ_T=1.45 g/cc, $\alpha=6.98\times10^5$ dyne/cm^2/(g/cc)^3, 70℃, v=0.6cm/sec, ρ(0)=0.15g/cc)

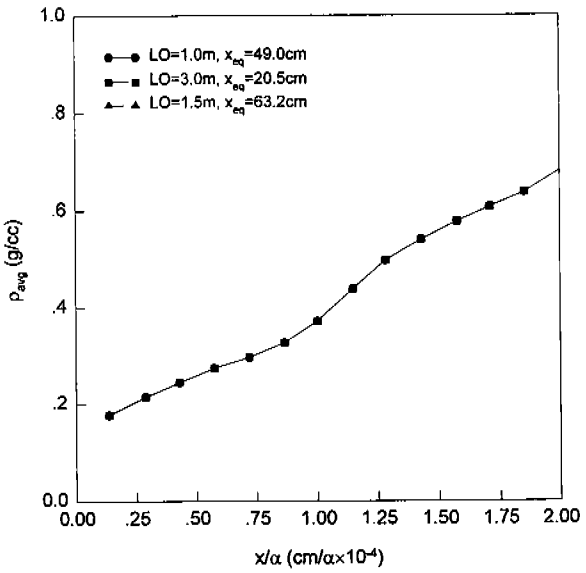

Fig. 7. Average density vs. depth/α at equillibrium for various tobacco bed heights. (ρ_T=1.45 g/cc, $\alpha=6.98\times10^5$ dyne/cm^2/(g/cc)^3, 70℃, v=0.6 cm/sec, ρ(0)=0.15 g/cc)

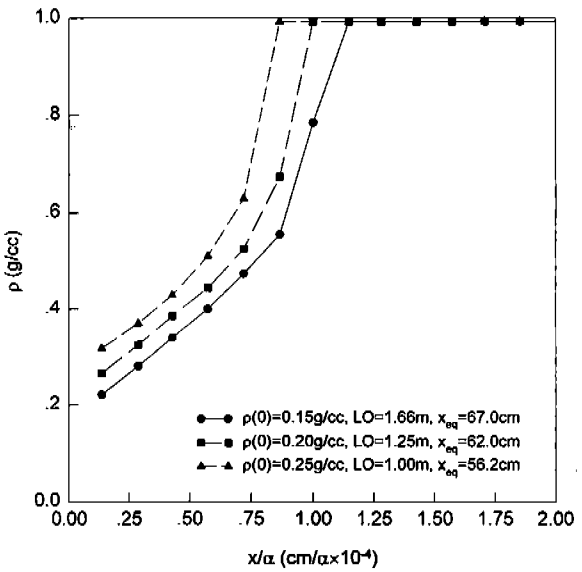

Fig. 8. Density vs. depth/α at equillibrium for various initial charge densities. (ρ_T=1.45 g/cc, $\alpha=6.98\times10^5$ dyne/cm^2/(g/cc)^3, 70℃, v=0.6 cm/sec, constant mass)

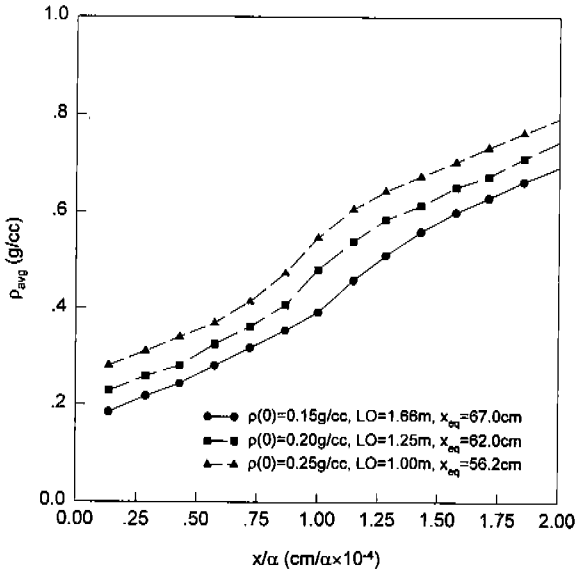

Fig. 9. Average density vs. depth/α at equillibrium for various initial charge densities. (ρ_T=1.45 g/cc, $\alpha=6.98\times10^5$ dyne/cm^2/(g/cc)^3, 70℃, v=0.6 cm/sec, constant mass)

dependence of compression (final depth) as critical as at 0.6 or 1.0 cm/sec. At a constant initial bed depth, the Figures show that density, average density, pressure gradient, and equilibrium depth increase as the initial tobacco bed density is increased from 0.15 to 0.25 g/cc. If initial bed density is maintained constant, while the initial bed depth is increases, the observables all increase as they did for density. However, if both initial density and height are varied to maintain a constant initial weight (charge), one observes that although density, average density, and pressure gradient increase, the equilibrium depth decreases as initial density increases.

The theory and experimental data for downflow show that there is a serious limitation to velocity and bed depth (unsupported) without using expensive internal support systems to allow stacking of shallow beds. The possibility of using upflow of CO_2 through the bed will be explored with the model.

Conclusions

A new model has been developed to describe the density and pressure gradient of supercritical CO_2 as a function of flow velocity through a vertical bed of tobacco. The model accounts for compaction of the tobacco by the combined effects of the flow, gravity, and buoyancy of the CO_2, which depend on CO_2 flow direction. A result of operating the process at temperatures in excess of the glass transition temperature of tobacco and at high moisture levels is a marked increase in the compressibility of the tobacco which leads to a severe dependence of the pressure gradient and tobacco density upon the flow velocity of the CO_2. At velocities in excess of 0.6 cm/sec at 70℃, there is a large increase in pressure gradient for beds deeper than about 0.5 meter (20 inches) for downflow.

At 70℃ the process can be operated at about 1.2 cm/sec at a nominal density of 0.15g/cc without any dependence upon tobacco bed weight. There would not be the severe compaction shown in the downflow case which will require stacking short (0.5 meter) beds. One could easily operate at bed depths of 1 - 3 meters and high flow velocities. The pressure and compaction will not be as severe as at 1.0 cm/sec obtained with downflow.

요 약

담배 고정층 반응기 내의 초임계 CO_2 압력 구배를 예측하는 수학적 모델을 개발하였다. 특히,

고정층 반응기 내의 담배의 압축율을 온도 및 CO_2의 속도의 함수로써 표현하였다. CO_2 가 하향 흐름인 경우에 대하여 개발된 모델을 적용함으로써 현상을 해석하였다. 온도가 70℃에서 CO_2 하향 속도가 0.6cm/sec를 초과했을 경우와 담배 고정층이 0.5m 보다 깊었을 경우에 심한 압력 구배를 보이는 것을 예측할 수 있다. 개발된 모델을 이용하면 초임계 CO_2 를 사용한 공정에서 많은 도움을 얻을 수 있다.

NOMENCLATURE

A bed cross sectional area (m^2)
a constant in Ergun's equation
b constabt in Ergun's equation
Dx incremental distance in a bed (m)
g gravity (m/sec^2)
K constant in equation (1)
LO initial bed height
P(x) mechanical pressure (pascal)
p local pressure in the tobacco bed (pascal)
p^* scaled pressure
RATM product ratio
V phase velocity of fluid (m/sec)
v fluid velocity (m/sec)
W_0 initial bed weight (kg)
x distance (m)
x^* scaled distance
xl bed height at position x (m)
xle final equilibrium bed depth (m)

Greek Letters

α constant in equation (4) $(dyne/cm^2)/(g/cc)^3$
ε_a true porosity
ε_b inerstitial porosity
ε_t total porosity
ρ tobacco bed density (kg/m^3)
ρ_a excluded volume density (kg/m^3)
ρ_{avg} average densty (kg/m^3)
ρ_{CO2} CO_2 density (kg/m^3)
ρ_i position density (kg/m^3)
ρ_m threshold density (kg/m^3)
ρ_{mt} mass density (kg/m^3)
ρ_0 initial density (kg/m^3)

References

1. Bird, R. B., W.E.Stewart, and E. N. Lighfoot (1960) Transport phenomena, p. 318, John Wiley & Sons, Inc., USA.
2. Simpson D.L. (1986) Private communications.